

# The influence of Titanium alloying and $\text{Co}_3\text{O}_4$ coating on the oxidation behavior of Fe-20Cr ferritic stainless steels for SOFC interconnects

A R Setiawan<sup>1</sup>, A. Ramelan<sup>2</sup>, R. Suratman<sup>3</sup> and A M Qizwini<sup>4</sup>

Research groups of Materials Engineering, Faculty of Mechanical and Aerospace Engineering, Institut Teknologi Bandung, Indonesia

E-mail: <sup>1</sup>asep.ridwans@material.itb.ac.id, <sup>2</sup>ramelan@material.itb.ac.id, <sup>3</sup>rochim@material.itb.ac.id, <sup>4</sup>alfizqizwini@gmail.com

**Abstract.** Ferritic steel is a potential metal candidate for interconnect solid oxide fuel cell (SOFC) because its ability to form chromia layer at the surface during high temperature operation. However, chromia based oxide scales is reluctant to the evaporation of Cr from the oxide-gas interface. In this work, a combination of titanium alloying and application of  $\text{Co}_3\text{O}_4$  spinel coating using dip coating method are carried out to improve the performance of ferritic steels as SOFC interconnect. The oxidation behavior of coated and uncoated Fe-20wt.%Cr alloys with different titanium contents: 0, 0.5, and 1 wt.% are studied as a function of time in air atmosphere. The samples were isothermally oxidized at 800°C for 24, 48, and 96 h in a box furnace. Preoxidation experiment were carried out on the alloys before the application of  $\text{Co}_3\text{O}_4$  coating to improve its adherence. X-ray diffraction analysis (XRD) and Scanning Electron Microscope (SEM) were used for characterization of the prepared samples. The results shows that increasing the concentration of titanium in the alloys both for coated and uncoated samples caused the increased oxidation rates. The oxidation resistance of  $\text{Co}_3\text{O}_4$  coated samples indicated from the weight change measurement was larger than that of the uncoated samples.  $\text{Co}_3\text{O}_4$  coating is not effective for improving the oxidation resistance of samples.

## 1. Introduction

Fuel cell are the electrochemical device which capable to convert chemical reaction energy directly into electrical energy without involves combustion. One of the attractive fuel cell technology is solid oxide fuel cell (SOFC). This type of fuel cell has gain popularity due to its low emission and high efficiency. A single SOFC cell usually consist of solid ceramic electrolyte, an electrode (anode and cathode) and interconnect components. YSZ ( $\text{Y}_2\text{O}_3$ -stabilized  $\text{ZrO}_2$ ) ceramics are typically used as an electrolyte for SOFC. The anode material is usually made from Ni-YSZ cermet, while the cathode is made from perovskite oxides, such as Sr-doped  $\text{LaMnO}_3$  (LSM).

<sup>1</sup> To whom any correspondence should be addressed.



Interconnect is one of the main components of planar type SOFC. The electrical connection between anode in one cell with the cathode in the adjacent cell are provided by the interconnect component. It is also function as a fuel separator. Due to its severe working condition, interconnect component must satisfy several criteria, such as high electrical conductivity, oxidation resistivity, gas permeability, etc. In the past, those criteria are met by ceramics materials such as lanthanum chromate ( $\text{LaCrO}_3$ ) [1]. These material are reported to have relatively high thermal stability and electrical conductivity in SOFC working condition at 1000 °C. However, ceramic interconnects are relatively difficult to fabricate and the cost is high. These factor become an obstacle for adoption in the industry, leading to the development of low cost metallic interconnects.

Recently, the operating temperature of solid oxide fuel cells (SOFC) are lowered from 1000 °C to 600-800 °C. The new condition has allowed the use of metallic material as interconnects. Among the various type of metal, ferritic steel is a potential candidate for SOFC interconnect because its ability to form continuous chromia layer at the surface during high temperature operation. Ferritic steels also offer several advantages for use as interconnect materials such as high mechanical strength, high thermal and electrical conductivity, CTE matching with other SOFC component and ease of fabrication. Despite these goods properties, these steels face many obstacle for adoption, such as unacceptably high oxidation rate, occurrence of buckling and spallation of the oxide scale when subjected to thermal cycling, and volatilization of high valence Cr-species in the form of  $\text{CrO}_3$ , or  $\text{Cr}(\text{OH})_2\text{O}_2$  which could lead to the degradation of overall cell performance [1,2]. The formation of oxide scale at the surface of ferritic steels will increase the contact resistance between electrodes and interconnect, reduce the SOFC cell efficiency.

Many studies have been done to improve the performance of ferritic steels as SOFC interconnect, from alloying design to surface treatments [1,3]. Several alloying element added to the ferritic steels such as Y, La, Ce [4] and Zr [5] are reported for improving oxidation resistance, scale adherence and conductivity. Small addition of element such as Nb, W, Ti, Mo to Fe-Cr alloys are effective to control the elemental diffusivities at the alloy grain boundaries by forming a laves type phase in air [6]. Nb, W and Mo addition to ferritic steels are also reported to improve the mechanical property, oxidation resistance, creep resistance and reduction of ASR [7,8]. Ti addition into ferritic steels was effective to reduce Cr evaporation [9-12]. However, if the amount of Ti is too high, oxidation rate and ASR will increase [10,12].

Protective coatings may also be utilize to improve the performance of ferritic steels. Several coating materials have been investigated extensively, such as perovskite ( $\text{LaSrCoO}_3$ ,  $\text{LaSrCrO}_3$ ,  $\text{LaSrMnO}_3$ ) and spinel ( $\text{MnCo}_2\text{O}_4$ ,  $\text{Mn}_{1.5}\text{Co}_{1.5}\text{O}_4$ ,  $(\text{Cu,Mn})_3\text{O}_4$ ) coating materials [3,13]. The coating are not effective to prevent diffusion of chromium outward [13]. In the previous work [11,12], the author have been investigated the oxidation behavior of Ti containing alloys at 700 and 800 °C in air atmosphere. The results indicated that the presence of Ti in the alloy increase the oxidation rate of Fe-20Cr alloy. In this work, a combination of titanium alloying and application of  $\text{Co}_3\text{O}_4$  spinel coating are carried out to improve the performance of Fe-20Cr during oxidation.

## 2. Experimental procedure

### 2.1. Sample preparation

Fe-20Cr alloy steels, with different titanium content; 0, 0.5 and 1 wt% were selected for the isothermal oxidation test at 800 °C. The chemical composition of chromium steels was analyzed using an Optical Emission Spectrometer (OES) ARL 3460. The results are shown in Table 1. Prior to oxidation, the specimens were cut into coupon with a size of 30 mm x 20 mm x 1 mm. After cutting, the surface of specimens were shot blasted using glass bead. Preoxidation experiment were carried out at 800 °C for 24 hour on the alloys before the application of  $\text{Co}_3\text{O}_4$  coating to improve its adherence. Then, the specimens were vertically dip coated in  $\text{Co}_3\text{O}_4$  slurries at room temperature. The slurries were prepared in a 250 ml beaker glass by adding 7 g  $\text{Co}_3\text{O}_4$  powder, 20 g ethanol and 1 g polyvinyl alcohol. The solution was stirred for one hour using magnetic stirrer at room temperature. The specimen were

then withdrawn from the solution slowly with constant speed after an approximate time of 30 seconds. Finally, after coating, the specimen were held vertically and dried at room temperature for 3 hour.

**Table 1.** Chemical composition of specimens (wt%).

	Fe	Cr	Ti	Mn	Si	C	P	S	V
Fe-20Cr	Bal	20.01	0.01	0.12	0.12	0.01	0.04	0.01	0.01
Fe-20Cr-0,5Ti	Bal	19.89	0.47	0.12	0.12	0.01	0.04	0.01	0.01
Fe-20Cr-1Ti	Bal	19.69	0.98	0.12	0.11	0.01	0.04	0.01	0.01

## 2.2. Oxidation test

For the isothermal oxidation test, as coated and uncoated specimen were oxidized at temperature of 800 °C for up to 345.6 ks in a muffle furnace. The steel samples were hang using stainless steel wire inside an alumina crucible. The crucible were placed inside the furnace and heated for periods of 86.4, 172.8, 345.6 ks. When the oxidation was terminated, the furnace was cooled down to a room temperature. In order to evaluate oxidation resistance, mass gain of specimen was measured with electronic balance before and after the oxidation. The oxidation kinetics can be calculated with parabolic kinetics law as follows:

$$(\Delta m / A) = k_p t \quad (1)$$

where  $\Delta m/A$  is mass gain per unit area,  $k_p$  is the parabolic rate constant,  $t$  is the oxidation time.

## 2.3. Analysis

After oxidation, the crystal structure of the oxide scale was identified by X-ray diffractometer (XRD) with CuK $\alpha$  radiation. The microstructure of oxide scale was characterized using scanning electron microscopy (SEM) with energy dispersive X-ray analysis (EDX).

# 3. Result and discussion

## 3.1. Oxidation behavior

Figure 1 and figure 2 shows the mass gain per unit area as a function of oxidation time, for all uncoated and coated steels during oxidation at 800 °C in air atmosphere. The oxidation behavior for all specimen, uncoated and coated Fe-20Cr, Fe-20Cr-0.5Ti and Fe-20Cr-1Ti alloy were followed the classical parabolic relationship with time. For uncoated specimen, Fe-20Cr alloys has the lowest mass change, followed by Fe-20Cr-0.5Ti and Fe-20Cr-1Ti. For Co<sub>3</sub>O<sub>4</sub> coated specimens, Fe-20Cr-0.5Ti has the lowest mass change, followed by Fe-20Cr, and Fe-20Cr-1Ti alloys. The presence of the Ti caused a significant changes in the oxidation resistance. The addition of titanium into the alloys increase the oxidation rate of Fe-20Cr alloy. Several researcher [4,14,15] reported that the presence of high amount of Ti in Cr<sub>2</sub>O<sub>3</sub> matrix may generated an excess ionic defect and reduced the oxidation resistance of the alloys. High amount of Titanium may induce the creation of additional cation vacancies in the Cr<sub>2</sub>O<sub>3</sub> matrix and subsequently promote fast diffusion of ion through Cr<sub>2</sub>O<sub>3</sub> layer. Compared to the bare specimens, the oxidation resistance of Co<sub>3</sub>O<sub>4</sub> coated samples indicated from the weight change measurement was larger. This indicated that Co<sub>3</sub>O<sub>4</sub> layer are not protective as Cr<sub>2</sub>O<sub>3</sub> in preventing oxygen inward diffusion into the substrate.

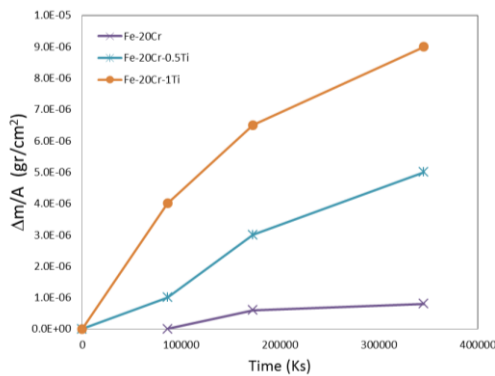


**Figure 1.** Oxidation behavior of Fe-20Cr with different titanium content : 0, 0.5 and 1 wt%.

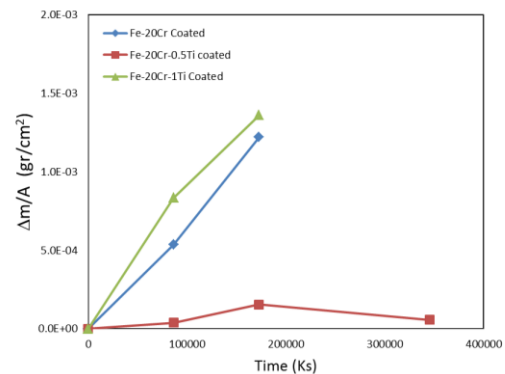


**Figure 2.** Oxidation behavior of Co<sub>3</sub>O<sub>4</sub> coated Fe-20Cr with different Titanium content: 0, 0.5 and 1 wt%.

The calculated parabolic rate constant for uncoated and coated Fe-20Cr, Fe-20Cr-0.5Ti and Fe-20Cr-1Ti alloys are shown in Table 2. For uncoated alloys, the addition of Ti element into Fe-20Cr increase the parabolic rate constants ( $k_p$ ) value 2 order of magnitude. In the case of Co<sub>3</sub>O<sub>4</sub> coated alloys, the addition of Ti element into Fe-20Cr increase the parabolic rate constants ( $k_p$ ) value 1 order of magnitude. Compared to the bare specimens, the parabolic rate constant of Co<sub>3</sub>O<sub>4</sub> coated samples was larger, 6 order of magnitude.

**Table 2.** Parabolic rate constant.

Alloys	Parabolic Rate Constant, $k_p$ ( $\text{gr}^2\text{cm}^{-4}\text{s}^{-1}$ )	
	Uncoated	Co <sub>3</sub> O <sub>4</sub> coated
Fe-20Cr	$2 \times 10^{-18}$	$8.6 \times 10^{-12}$
Fe-20Cr-0.5Ti	$7 \times 10^{-17}$	$1.1 \times 10^{-11}$
Fe-20Cr-1Ti	$2 \times 10^{-16}$	$2.1 \times 10^{-11}$

### 3.2. Phase identification

The XRD profile of the oxide scale formed on the uncoated specimen surface after 96 h oxidation at 800 °C is shown in figure 3.

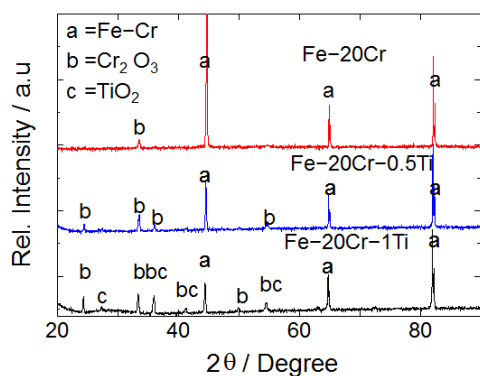


**Figure 3.** XRD Profile of uncoated Fe-20Cr, Fe-20Cr-0.5Ti and Fe-20Cr-1Ti alloy after oxidation at 800 °C for 96 hour.

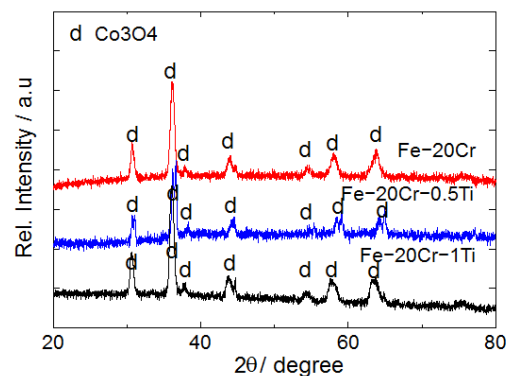


**Figure 4.** XRD Profile of Co<sub>3</sub>O<sub>4</sub> coated Fe-20Cr, Fe-20Cr-0.5Ti and Fe-20Cr-1Ti alloy after oxidation at 800 °C for 96 hour.

Strong peaks of  $\text{Cr}_2\text{O}_3$  are observed in all alloys. The presence of  $\text{TiO}_2$  are detected on Fe-20Cr-0.5Ti and Fe-20Cr-1Ti alloy. The peak of alpha iron (Fe-Cr) in Ti containing alloys, decreases, indicating that the oxide scales was thicker so that X-ray penetration into the substrate are limited. The formation of  $\text{TiO}_2$  and  $\text{Cr}_2\text{O}_3$  in Fe-20Cr-0.5Ti and Fe-20Cr-1Ti alloy increases the mass gain of the alloys during oxidation.

The XRD profile of  $\text{Co}_3\text{O}_4$  coated specimen after 96 hour oxidation at 800 °C are displayed in figure 4. Strong peaks of  $\text{Co}_3\text{O}_4$  are observed in all alloy.  $\text{Cr}_2\text{O}_3$  and  $\text{TiO}_2$  phase were not detected on the XRD profile. This is due to very thick  $\text{Co}_3\text{O}_4$  scales formed in the surface, so that the X-ray penetration into the substrate are limited.

### 3.3. Oxide morphology of $\text{Co}_3\text{O}_4$ coated specimen

Cross-section morphology of  $\text{Co}_3\text{O}_4$  coated specimen after oxidation test was observed using Scanning electron microscope (SEM), as shown in figure 5. Thick oxide layer were found on the top surface, composed mainly of  $\text{Co}_3\text{O}_4$ . The oxide layers are porous. In Fe-20Cr-0.5Ti and Fe-20Cr-1Ti alloy,  $\text{TiO}_2$  oxides were precipitated internally at the alloy/oxide interfaces. The results are similar with our previous work [11,12].

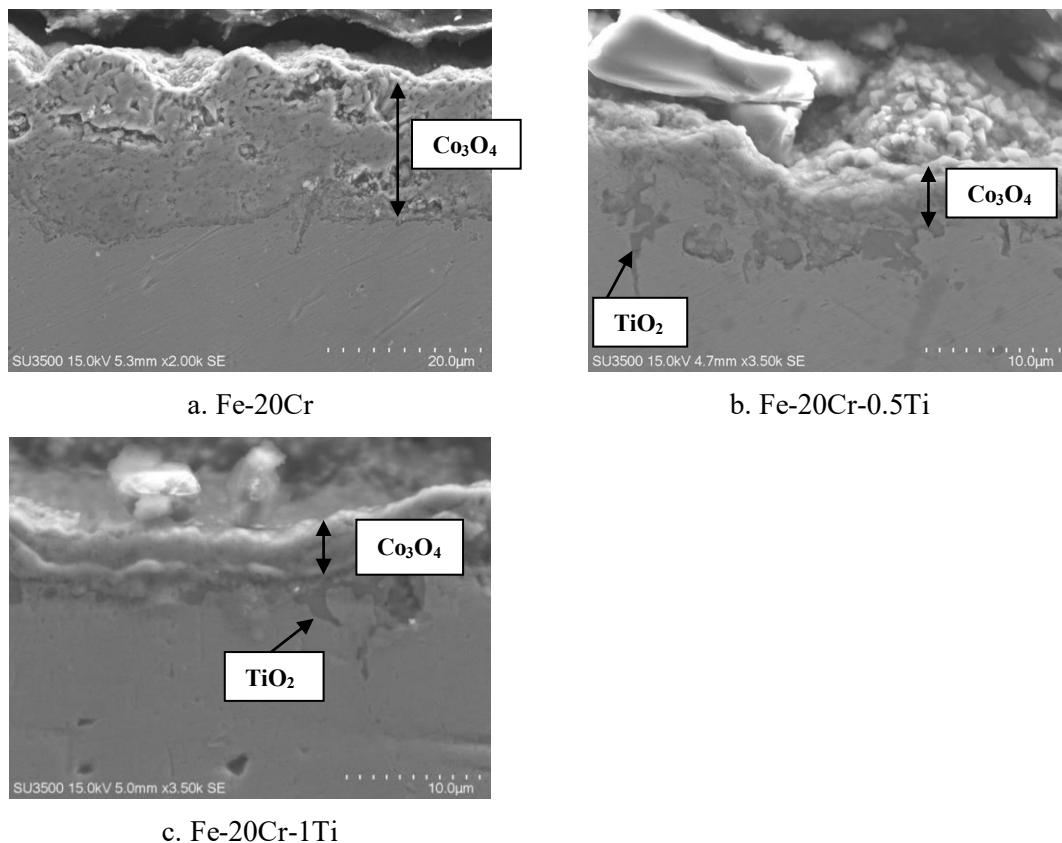


**Figure 5.** Cross section morphology of  $\text{Co}_3\text{O}_4$  coated specimen after oxidation at 800 °C for 96 hour in air atmosphere.

The amount of Ti in Fe-20Cr alloy was not enough to form continuous  $\text{TiO}_2$  layers in the surface of alloys. The formation of  $\text{TiO}_2$  oxide at the oxide/alloy interfaces indicated that the  $\text{Co}_3\text{O}_4$  layer were not protective, so that oxygen from the atmosphere diffuse inward to react with Ti element in the substrate to form  $\text{TiO}_2$  oxide. As a result, the oxidation behavior of Fe-20Cr-0.5Ti and Fe-20Cr-1Ti alloys increased significantly compared to the Fe-20Cr alloy, both for bare and coated alloy. Detail observation on the oxide morphology also indicated that the presence of Ti element in Fe-20Cr alloy

may cause higher rate of spallation. High amount of Ti oxide in the interface formed the void and reduced the adhesion of the oxide to the substrate [16].

#### 4. Conclusion

Investigation on the oxidation behavior of uncoated and  $\text{Co}_3\text{O}_4$  coated Fe-20Cr, Fe-20Cr-0.5Ti and Fe-20Cr-1Ti alloys indicated that the alloy are still far from the application as SOFC interconnect. The oxidation test clearly indicated that Ti addition into Fe-20Cr alloy, both for coated and uncoated specimen, increases the oxidation rate of the alloy significantly. This is supported from SEM observation. In Ti containing alloys, large amount of Ti-oxide was dispersed in the oxide/metal interface and led to internal oxidation. The oxidation resistance of  $\text{Co}_3\text{O}_4$  coated samples indicated from the weight change measurement was larger than that of the uncoated samples.  $\text{Co}_3\text{O}_4$  layer is porous, and not effective for improving the oxidation resistance of samples

#### 5. Reference

- [1] Zhu W Z and Deevi S C 2003 *Mat. Sci. Eng. A* **348** 227
- [2] Zhu W C and Deevi S C 2003 *Mater. Res. Bull.* **38** 957.
- [3] Shaigan N, Qu W, Ivey D G and Chen W 2010 *J. Power. Sources.* **195** 1529
- [4] Seo H S, Jin G, Jun J H, Kim D-H and Kim K Y 2008 *J. Power. Sources.* **178** 1
- [5] Hua B, Pu J, Lu F, Zhang J, Chi B and Jian L 2010 *J. Power. Sources.* **195** 2782
- [6] Wu J, S. Gemmen R, Manivannan A and Liu X 2011 *Int. J. Hydrogen. Energ.* **36** 4525
- [7] Yun D W, Seo H S, Jun J H, Lee J M and Kim K Y 2012 *Int. J. Hydrogen. Energ.* **37** 10328
- [8] Yun D W, Seo H S, Jun J H and Kim K Y 2013 *Int. J. Hydrogen. Energ.* **38** 1560
- [9] Seo H S, Yun D W and Kim K Y 2012 *Int. J. Hydrogen. Energ.* **37** 16151
- [10] Jablonski P D and Alman D E 2008 *J. Power. Sources.* **180** 433
- [11] Setiawan A R and Artono T J 2016 *AIP. Conf. Proc.* **1711** 040003
- [12] Ruhma Z, Setiawan A R, Ramelan A and Suratman R 2014 *Appl. Mech. Mater.* **660** 249
- [13] Bi Z H, Zhu J H and Batey J L 2010 *J. Power. Sources.* **195** 3605
- [14] Geng S and Zhu J 2006 *J. Power. Sources.* **160** 1009
- [15] Holt A and Kofstad P 1999 *Solid State Ionics* **117** 21
- [16] Safikhani A, Esmailian M, Tinatiseresht T and Darband G B 2016 *Int. J. Hydrogen. Energ.* **41** 6045–52